

ATCA and CMB anisotropies

Ravi Subrahmanyan

*Australia Telescope National Facility, CSIRO, Locked bag 194, Narrabri,
 NSW 2390, Australia*

Abstract. Australia Telescope Compact Array (ATCA) observations in sky regions selected to be low in foreground confusion have been used to infer limits on arcmin-scale CMB anisotropy in total intensity and polarization. These deep searches have, hitherto, been made using the East-West ATCA in an ultra-compact 1-D array configuration and in the highest available frequency band at 3-cm wavelength. The ATCA is being upgraded for operation at mm wavelengths and in 2-D array configurations: the enhanced capabilities present a new opportunity for pursuing CMB anisotropy related observations with reduced foreground confusion and at smaller angular scales.

1. Introduction

Observations of primary cosmic microwave background (CMB) anisotropies and estimates of the angular spectrum of the anisotropies, when compared with predictions for these spectra based on structure formation theory and the propagation of the CMB photons through growing matter perturbations in the recombination era and at later times, have long been expected to provide us with useful estimates of the cosmological parameters and the primordial perturbation spectrum (see, for example, Bond, Efstathiou, & Tegmark 1997). In a spherical harmonic decomposition of the CMB anisotropy, the primary anisotropy spectrum is expected to be exponentially cut off at multipole orders l exceeding about 2500 (Hu & White 1997). At higher multipoles — at arcmin and smaller angular scales — the CMB spectrum is expected to be dominated by secondary effects: anisotropy owing to the Sunyaev-Zeldovich effect (SZE; see, for example, Refregier et al. 2000 and references therein) in a cosmological distribution of hot gas in cluster potential wells is predicted to be the most important contributor. The CMB is also expected to be fractionally polarized — the polarization has to date not been detected — and any measurements of the angular spectrum in polarization modes or the correlation between polarization anisotropy and that in total intensity would provide additional constraints on cosmology and help resolve certain parameter degeneracies (Seljak & Zaldarriaga 1997).

2. Australia Telescope CMB results to date

The Australia Telescope Compact Array (ATCA; see The Australia Telescope 1992) is located at Narrabri in Australia, has five 22-m diameter antennae mov-

able along a 3-km East-West railtrack, a sixth antenna stationed 3 km from the end of the track, and usually operates as an interferometric Fourier Synthesis array. The array was commissioned with 20, 13, 6 and 3-cm capability and has been in operation for more than a decade.

CMB anisotropy searches using the ATCA have, so far, been made at the highest available frequency band of 3-cm where foreground confusion is lowest. To maximize the array brightness sensitivity, the five antennas were close-packed into a 1-D East-West 122-m array in which the antennas were equi-spaced 30.6 m apart. Shadowing results in spurious responses at the ATCA (Subrahmanyam 2002) and, therefore, fields were selected at declinations close to -50° to avoid shadowing. At this declination, the projected antenna spacing is close to the antenna diameter for a large hour angle range and observations at this declination have the best brightness sensitivity (without shadowing).

Fields were observed in full Earth-rotation Fourier synthesis mode and the strategy has been to examine images of the fields synthesized from the visibility data for any CMB anisotropy. The five-antenna 122-m array gives 30.6-m spacing visibilities on four baselines; the remaining six baselines have spacings from 61 to 122 m. Images synthesized using exclusively the four 30.6-m baselines have the highest brightness sensitivity: these images are the most sensitive to flat-band CMB anisotropy. The longer baselines are relatively insensitive to flat-band anisotropies; however, they respond to foreground discrete sources which are unresolved on those baselines. Therefore, the strategy has been to use images made using the six longer baseline data to estimate the foreground discrete source confusion in the fields and use images made using the four 30.6-m baselines for CMB anisotropy searches. Stokes I, Q & U images were examined for any CMB anisotropy. The Stokes V images served as an estimator of the instrument thermal noise.

In Subrahmanyam et al. (1993) were reported results based on observations of a single field at 8.7 GHz. This was followed by a deeper integration on the single field, along with observations of the foreground confusion at a lower frequency of 4.8 GHz in a roughly scaled array in which the five antennas were equi-spaced 61-m apart to form a 244-m array (Subrahmanyam et al. 1998).

Results from deep observations of six separate fields at 8.7 GHz are in Subrahmanyam et al. (2000). These six fields had been selected to be low in foreground discrete sources based on lower frequency ATCA observations. The fields were observed for about 50 hr each and the 2-arcmin resolution images, which were made using exclusively the 30.6-m baselines, had rms thermal noise of $24 \mu\text{Jy beam}^{-1}$: this was as expected given the observing parameters and telescope system temperatures. The telescope filter function, corresponding to the CMB sky variance as estimated from primary-beam weighted image pixels, peaks at multipole $l = 4900$ and has half-maximum values at $l = 3520$ and 6200 . Each of the six 2-arcmin resolution images has about 2π independent pixels and the six images together represent 12π independent estimates of the CMB sky as viewed through this telescope filter function. A flat-band CMB anisotropy spectrum with normalization $Q_{flat} \mu\text{K}$ is expected to result in an image rms $0.844Q_{flat} \mu\text{Jy beam}^{-1}$; consequently, the image thermal noise corresponds to $28 \mu\text{K}$.

2.1. Results on polarization anisotropy

The Stokes Q and U images of all six fields were consistent with the expectations from thermal noise. The image rms, estimated using pixels in all the six images with appropriate weights, was 22.2 and 21.8 $\mu\text{Jy beam}^{-1}$ in Stokes Q and U respectively. No polarization anisotropy is detected and, using the likelihood ratio test, upper limits of $Q_{flat} < 11$ and 10 μK are derived, respectively, for Stokes Q and U CMB anisotropy in the ATCA filter function.

2.2. Results for total intensity anisotropy

The rms of the sky intensity fluctuations in Stokes I, estimated using all the six images, was 117 $\mu\text{Jy beam}^{-1}$; there was significant ‘excess’ image variance above that expected from the telescope thermal noise. The higher resolution images made using visibilities with baselines in the 61-122 m range showed obvious foreground discrete sources in the fields. The foreground confusion was modelled using the long baseline data — the model derived consisted of 0-4 ‘point’ sources in each field with flux density up to 455 $\mu\text{Jy beam}^{-1}$ — and the model was subtracted. The image rms derived from the residual images was 52 $\mu\text{Jy beam}^{-1}$ and this was also significantly in excess of the thermal noise.

The residual confusion in the residual images was estimated via simulations. The differential source counts at 8.7 GHz, derived from deep VLA observations by Windhorst et al. (1993), was used to generate simulated sky images containing the expected thermal noise and discrete sources. The images were processed in a pipeline which simulated the observing strategy and data processing including the identification of confusion from the long-baseline data. The simulated residual images were used to derive the distribution for the estimate of the residual image rms. The simulations suggested that the residual weak-source confusion may cause the residual images to have rms 51-66 $\mu\text{Jy beam}^{-1}$ ($1\text{-}\sigma$ spread). This estimate is consistent with the observational results and, therefore, we have been led to believe that the ‘excess’ variance in the residual images, following the subtraction of the confusion model, is owing to weak unsubtracted confusion and not CMB anisotropy.

Assuming that thermal noise and discrete source confusion (including weak confusion from sources not identified in the long-baseline data) are the only contributors to the image apart from any flat band CMB anisotropy, a likelihood ratio test gave upper limits of $Q_{flat} < 25 \mu\text{Jy beam}^{-1}$ with 95 per cent confidence.

3. ATCA mm upgrade

The ATCA is being upgraded for mm operations. All five movable antennae are being fitted with 12 and 3 mm receivers covering the bands 16-25 and 85-115 GHz. The receivers are being built around Indium Phosphide MMIC low-noise amplifiers which are designed in-house at the Australia Telescope National Facility (ATNF) laboratories in Sydney. Prototype receivers installed on two antennae have receiver temperatures (measured at the face of the feed horns) of about 25 and 100 K respectively at 21 and 95 GHz; the system temperatures

are 45 and 175 K at these frequencies. Temperatures in the 3 mm band are expected to improve in later versions.

The antenna surfaces have been upgraded for mm operations: panels with perforations have been replaced with solid panels which have $< 100 \mu\text{m}$ rms errors and holography has been used to reset the panels. The receiver feed horns illuminate the entire 22-m aperture of the antennae even at 3 mm: the ATCA antennas have shaped reflectors for the Cassegrain optics and the aperture illumination is fairly uniform out to the edges and this gives the short-baseline interferometers good brightness sensitivity. Because the peripheral regions of the antenna surfaces are important for brightness sensitivity, the holographic panel setting used a feed horn which over illuminated the edges and improved sensitivity for locating the outer panels. All these imply that the ATCA has good brightness sensitivity and this is important for CMB related work.

The atmosphere is a significant degrader of system temperature particularly at mm wavelengths; therefore, observations are better done at high elevations. In order to have good visibility-plane coverage from observations at exclusively high elevations and short durations, the upgrade includes the addition of a North-spur to the current East-West railtrack. CMB observations with the ATCA have, in the past, been made with 1D close-packed arrays. The brightness sensitivity of an interferometric array is better if the array configuration is close-packed in 2D. The upgrade makes it possible for CMB observations with the ATCA, in future, to be made in 2D configurations.

A separate project, which is also part of the upgrade, is a redesign of the phase transfer system to provide phase-stable reference local oscillators at each antenna of the interferometer array for down-conversion of the high frequencies without loss of coherence.

A related development, which is expected to come off in the next few years, is an upgrade of the ATCA correlator to wider bandwidths. The increase from the current 2×128 MHz to several GHz will vastly enhance the continuum sensitivity of the interferometer: this is vital for CMB anisotropy related observations where sky signals are extremely weak.

4. Prospects for ATCA CMB observations in the future

Many CMB anisotropy related observations are now being made at mm wavelengths, about 100 GHz, where confusion from synchrotron and dust foregrounds are believed to be lowest. The focus is also shifting to smaller angular scales and here the errors in the estimates of the CMB power spectrum may be dominated by discrete source confusion. However, all estimates of source counts at mm wavelengths are based on mm observations of sources detected in cm wavelength surveys: there are no surveys which cover significant sky areas at mm wavelengths. The 3-mm capability in the upgraded ATCA may make a useful contribution in de-confusing CMB surveys. It may be noted here that the region of the sky which is lowest in dust emission is in the vicinity of the south Galactic pole, in the southern sky, and this is where many current CMB anisotropy searches are being directed. The ATCA is the only mm interferometer capable of observing this region today and the upgraded telescope may play a role in

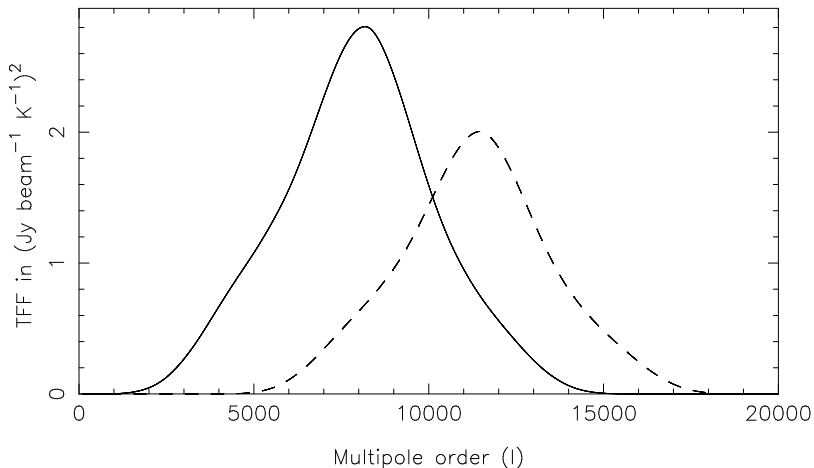


Figure 1. Telescope filter functions for a single ATCA baseline at 18 GHz. The continuous line is for a projected baseline of 22 m; the dashed line is for 30.6 m.

detecting and monitoring the stronger discrete sources in the CMB fields for de-confusing total intensity or polarization anisotropy observations.

In any ultra-compact array configuration, assuming that the system temperature and other observing parameters remain the same, and for frequencies in the Rayleigh-Jeans regime ($h\nu \ll kT_o$; where $T_o = 2.726$ K), the ATCA sensitivity to flat-band CMB anisotropy does not change with the observing frequency. The interferometer response, in Jy beam^{-1} , is the same for a fixed Q_{flat} or for a flat spectrum with $l(l+1)C_l/(2\pi)$ a constant.

However, primary anisotropies are believed to cut off beyond about $l \sim 2500$ and SZE anisotropy searches with angular resolutions much better than an arcmin are not currently considered useful; therefore, anisotropy searches with the upgraded ATCA may be made at the lower end of the 12 mm band, around 16-20 GHz. The telescope filter function, corresponding to an interferometer consisting of two 22-m ATCA antennas spaced 30.6 m apart, is given in Figure 1. The continuous curve gives the filter corresponding to a projected baseline of 22 m, the dashed line gives the filter corresponding to a projected baseline of 30.6 m; both curves have been computed assuming operation at 18 GHz. The telescope response peaks at l in the range 8000-12000 depending on the foreshortening of the baseline in projection. Assuming that at arcmin scales, the secondary CMB anisotropy may be described by a flat band CMB anisotropy spectrum, I find that for $\sqrt{l(l+1)C_l/(2\pi)} \times 2.726 \text{ K} = 10 \mu\text{K}$, the expected signal is $10 \mu\text{Jy beam}^{-1}$ when the ATCA baseline is 30.6 m and $14 \mu\text{Jy beam}^{-1}$ when the projected baseline is 22 m.

The extragalactic discrete source confusion would be very much reduced at the higher frequencies available following the upgrade. If we adopt a differential source count which scales with the flux density S and frequency ν as

$$N(S) \sim S^{-2.18} \nu^{-0.8\alpha}, \quad (1)$$

where $\alpha = 0.7$ is the spectral index (defined by the relation $S_\nu \sim \nu^{-\alpha}$), the integral source count obeys the scaling relation:

$$N(> S) \sim S^{-1.18} \nu^{-0.56} \Omega, \quad (2)$$

where Ω is the beam solid angle (which scales with frequency as ν^{-2}). The confusion limit may be taken to be the flux density S_c at which $N(> S_c) \approx 1$; it follows that the confusion limit scales with frequency as $S_c \sim \nu^{-2.17}$. As compared to previous ATCA CMB observations at 8.7 GHz, any future observations at 18 GHz, with identical observing strategy, would have a confusion that is lower by factor 5.

Acknowledgments. The Australia Telescope is funded by the Commonwealth of Australia for operation as a National facility managed by CSIRO.

References

- Bond, J. R., Efstathiou, G., & Tegmark, M. 1997, MNRAS, 291, L33
- Hu, W., & White, M. 1997, ApJ, 479, 568
- Refregier, A., Komatsu, E., Spergel, D. N., & Pen, U. L. 2000, Phys.Rev.D, 61, 79
- Seljak, U., & Zaldarriaga, M. 1997, Phys.Rev.Lett, 78, 2054
- Subrahmanyan, R., Ekers, R. D. E., Sinclair, M., & Silk, J. 1993, MNRAS, 263, 416
- Subrahmanyan, R., Kesteven, M. J., Ekers, R. D. E., Sinclair, M., & Silk, J. 1998, MNRAS, 298, 1189
- Subrahmanyan, R., Kesteven, M. J., Ekers, R. D. E., Sinclair, M., & Silk, J. 2000, MNRAS, 315, 808
- Subrahmanyan, R. 2002, in AIP Conf. Proc., 2K1BC workshop on Experimental Cosmology at millimetre wavelengths held at Breuil-Cervinia, Italy, July 2001, ed. M. De Petris & M. Gervasi (New York: AIP)
- The Australia Telescope, 1992, special issue of J. Electr. Electron. Eng. Aust., 12, June
- Windhorst, R. A., Miley, G. K., Owen, F. N., Kron, R. G., Koo, D. C. 1995, ApJ, 289, 494